HHS Public Access

Author manuscript

Ann Neurol. Author manuscript; available in PMC 2018 June 01.

Published in final edited form as:

Ann Neurol. 2017 June ; 81(6): 790–803. doi:10.1002/ana.24946.

Rabies Tracing of Birthdated Dentate Granule Cells in Rat Temporal Lobe Epilepsy

Xi Du[1,2], **Helen Zhang**[3], and **Jack M. Parent**[1,2,3]

[1]Neuroscience Graduate Program, University of Michigan Medical Center and Ann Arbor VA Healthcare System, Ann Arbor, Michigan, USA

[2]Medical Scientist Training Program, University of Michigan Medical Center and Ann Arbor VA Healthcare System, Ann Arbor, Michigan, USA

[3]Department of Neurology, University of Michigan Medical Center and Ann Arbor VA Healthcare System, Ann Arbor, Michigan, USA

Abstract

Objective—To understand how monosynaptic inputs onto adult-born dentate granule cells (DGCs) are altered in experimental mesial temporal lobe epilepsy (mTLE) and whether their integration differs from early-born DGCs that are mature at the time of epileptogenesis.

Methods—A dual-virus tracing strategy combining retroviral birthdating with rabies virus-mediated putative retrograde trans-synaptic tracing was used to identify and compare presynaptic inputs onto adult- and early-born DGCs in the rat pilocarpine model of mTLE.

Results—Our results demonstrate that hilar ectopic DGCs preferentially synapse onto adult-born DGCs after pilocarpine-induced status epilepticus (SE) while normotopic DGCs synapse onto both adult- and early-born DGCs. We also find that parvalbumin+ and somatostatin+ interneuron inputs are greatly diminished onto early-born DGCs after SE. However, somatostatin+ interneuron inputs onto adult-born DGCs are maintained, likely due to preferential sprouting. Intriguingly, CA3 pyramidal cell backprojections that specifically target adult-born DGCs arise in the epileptic brain, while axons of interneurons and pyramidal cells in CA1 appear to sprout across the hippocampal fissure to preferentially synapse onto early-born DGCs.

Interpretation—These data support the presence of substantial hippocampal circuit remodeling after an epileptogenic insult that generates prominent excitatory monosynaptic inputs, both local recurrent and widespread feedback loops, involving DGCs. Both adult- and early-born DGCs are targets of new inputs from other DGCs as well as from CA3 and CA1 pyramidal cells after pilocarpine-treatment, changes that likely contribute to epileptogenesis in experimental mTLE.

Corresponding author: Jack M. Parent, M.D., Address: Dept. of Neurology, 5021 BSRB, 109 Zina Pitcher Place, Ann Arbor, MI 48109-2200. Telephone: 734-763-3776, Fax: 734-763-7686, parent@umich.edu.

AUTHOR CONTRIBUTIONS

XD, HZ and JMP contributed to the conception and design of the study; XD contributed to the acquisition and analysis of the data; XD and JMP contributed to drafting the text and preparing the figures.

POTENTIAL CONFLICTS OF INTEREST

Nothing to report.

Keywords

Seizure; hilar ectopic; adult neurogenesis; neural stem cells; epileptogenesis

INTRODUCTION

Mesial temporal lobe epilepsy (mTLE) is estimated to afflict over 25 percent of adults diagnosed with epilepsy.[1] The pathological hallmarks are hippocampal cell loss and gliosis,[2] changes that are recapitulated in the rat pilocarpine mTLE model.[3,4] Although mTLE pathogenesis remains poorly understood, accumulating evidence implicates aberrant hippocampal dentate gyrus plasticity in this process. In human and experimental mTLE, dentate granule cells (DGCs) demonstrate characteristic morphological abnormalities such as mossy fiber sprouting, persistent hilar basal dendrites, granule cell layer dispersion and ectopic soma placement.[5–11] DGCs are also the only hippocampal neurons that continue to be generated throughout adulthood[12] and adult DGC neurogenesis is robustly potentiated by seizures.[7] Dentate gyrus structural changes after chemoconvulsant-induced status epilepticus (SE) are thought to largely arise from the aberrant development of the adult-born DGC population.[13–16] However, recent work indicates that pre-existing DGCs also contribute to mossy fiber sprouting.[17]

Adult-born DGCs are implicated as the major source of hilar ectopic DGCs and DGCs with basal dendrites, both of which have been proposed to be ‘hub’ cells with excitatory hyper-connectivity.[15,16,18,19] Previous work has focused on the postsynaptic targets of DGCs generated after SE[20,21] with less knowledge about how their synaptic inputs change during epileptogenesis. This question is especially crucial in light of the mounting evidence that network remodeling in the epileptic brain is much more extensive than previously believed. Seizure-induced hippocampal synaptic reorganization not only involves excitatory neurons[5,17,22,23] but also surviving interneurons.[19,24–26] Understanding whether excitatory and inhibitory sprouting is preferentially onto the pre-existing or newly-born DGC population should provide important clues as to how pro-seizure networks develop after an epileptogenic insult.

To determine if pilocarpine-induced SE differentially influences the plasticity of adult-born versus pre-existing DGCs, we employed a dual-viral tracing strategy combining retroviral (RV) birthdating with rabies virus (RbV)-mediated putative retrograde trans-synaptic tracing.[27] This approach was used to study first-order monosynaptic inputs onto adult- and early-born DGCs in the chronically epileptic or intact brain. We found a striking degree of feedback/recurrent excitatory input onto both populations after SE, including direct pyramidal cell to DGC projections from CA3 and CA1, with differential changes in inhibitory inputs onto these two age-defined DGC populations. These results suggest that DGCs receive widespread local and long-distance monosynaptic excitation that likely contributes to epileptogenesis in experimental mTLE.

MATERIALS AND METHODS

Viral Production

We generated a RV construct (RV-Syn-GTR) consisting of a Murine Moloney Leukemia virus-based RV vector containing a human Synapsin1 promoter driving GFP, the avian sarcoma leukosis virus receptor TVA and RbV glycoprotein (Rgp). To make pSyn-eGFP-TVA-Rgp-WPRE (pSyn-GTR), the GTR DNA fragment was obtained by PCR from the pBOB-SynP-HTB template (a gift from Edward Callaway, Salk Institute, La Jolla, CA) and used to replace GFP in pCAG-GFP-WPRE (a gift from Fred Gage, Salk Institute). A control RV (con-RV) was generated by deleting Rgp from pSyn-GTR. Pseudotyped RV stocks were produced by co-transfecting RV constructs with VSV-G plasmid into the GP2-293 packaging cell line (Clontech, CA). Harvested supernatant containing RV was filtered through a 0.45 μM filter (Gelman Sciences, MI) and concentrated by ultracentrifugation. Titers ranged from 2–5 × 10^8 cfu/mL. An mCherry (mCh)-expressing, avian envelope glycoprotein subgroup A (EnvA)-pseudotyped RbV (RbV-mCh) was produced as described previously[28] with titers of 2–4 × 10^5 cfu/mL used. Lentivirus (CAMKIIα-Syp-GFP) was generated by transient transfection of the following plasmids: translt-LT1 (Mirus Bio, Madison, WI), vector, psPAX2 and pMD2.G. Supernatant was harvested 48 hours later, filtered and concentrated by ultracentrifugation.

Animals

All animal procedures were performed following protocols approved by the Institutional Animal Care and Use Committee of the University of Michigan and in accordance with the U.S. Public Health Service's Policy on Humane Care and Use of Laboratory Animals. Animals were purchased from Charles River and maintained under a constant 12 h light/dark cycle with access to food and water *ad libitum.* A total of 248 animals underwent pilocarpine-induced SE or sham treatment in this study and 36 animals were used for the final experimental analyses. Approximate numbers of animals excluded during the sequence of procedures includes: 20% loss from pilocarpine treatment; 35% death from one of the two viral injections; 25% from unsuccessful targeting of viral injections; and 5% exclusion due to grossly damaged dentate gyri from injection or SE. Epileptic and sham control rats were generated as previously described.[15,17] Briefly, adult male Sprague Dawley rats at postnatal day (P) 56 were pretreated with atropine methylbromide (5 mg/kg i.p.; Sigma-Aldrich, St. Louis, MO) and 20 minutes later received the chemoconvulsant pilocarpine hydrochloride (340 mg/kg, i.p.; Sigma-Aldrich). Seizures were monitored behaviorally and terminated with diazepam (10 mg/kg, i.p.; Hospira Inc., Lake Forest, IL) after 90 minutes of SE. Seizure severity was scored on the standard Racine scale[29] and all SE animals reached a score of 5 (with multiple events of rearing and falling with forelimb clonus). Controls received identical treatment except pilocarpine was replaced with 0.9% saline.

Intrahippocampal Injections

To birthdate early- or adult-born DGCs and render them RbV-competent, RV-Syn-GTR (expressing GFP, TVA, and Rgp) was injected bilaterally into the dorsal dentate gyrus at either P7 or P60, respectively, as described previously.[15,17] Briefly, P7 pups were anesthetized on ice and placed on a neonatal rat stereotaxic adapter (Stoelting, Wood Dale,

IL) in a Kopf stereotaxic frame (Tujunga, CA). Bilateral burr holes were drilled and 1 μL of RV-Syn-GTR was injected (0.1 μL/min) using a 5 μL Hamilton syringe with the following coordinates (in mm from bregma and mm below the skull): caudal 2.0, lateral 1.5, depth 2.7. P60 rats were anesthetized with Ketamine/Xylazine and placed in a Kopf stereotaxic frame. Bilateral burr holes were drilled and 2 μL of RV-Syn-GTR (or con-RV; Fig 2) was injected as for P7 pups except the following coordinates (in mm from bregma and mm below the skull) were used: caudal 3.9, lateral 2.3, depth 4.2.

To trace monosynaptic inputs onto RV-Syn-GTR-infected, birthdated DGCs, RbV-mCh was injected bilaterally into the dorsal dentate gyrus at 8–10 weeks after pilocarpine or vehicle treatment (P112-126). Animals were anesthetized using Ketamine/Xylazine and placed in a stereotaxic frame. Bilateral burr holes were drilled and 2 μL of RbV-mCh was injected (0.1 μL/min) at the following coordinates (in mm from bregma and mm below the skull): caudal 4.2, lateral 2.3, depth 4.2.

To label CA1 pyramidal cell axons/synaptic terminals in separate experiments, a lentivirus carrying a CAMKIIα promoter driving a synaptophysin-GFP fusion gene (CAMKIIα-Syp-GFP) was injected bilaterally into hippocampal CA1 at 3 weeks after SE or sham treatment (P77). Animals were anesthetized using Ketamine/Xylazine and 1 μL of CAMKIIα-Syp-GFP was injected (0.1 μL/min) using the following coordinates (in mm from bregma and mm below the skull): caudal 3.8, lateral 2.0, depth 2.5.

Immunohistochemistry

One week after injection of RbV-mCh or CAMKIIα-Syp-GFP, animals were deeply anesthetized with pentobarbital and transcardially perfused with 0.9% saline followed by 4% paraformaldehyde (PFA). Brains were removed and post-fixed overnight at 4°C in 4% PFA and cryoprotected. Frozen coronal sections (40 μm thickness) were cut using a sliding microtome. Series' of 12–16 sections (480 μm apart) were processed for immunofluorescence histochemistry (double- and triple-labeling) using the following primary antibodies: chicken anti-GFP (1:1000, Aves), rabbit (Rb) anti-dsRed (1:1000, Clontech), mouse (Ms) anti-mCherry (1:1000, Clontech), Rb anti-Prospero Homeobox 1 (Prox1; 1:1000, a gift from Sam Pleasure, University of California, San Francisco, San Francisco, CA), Ms anti-Parvalbumin (PV; 1:400, Sigma), or Rb anti-Somatostatin (SST; 1:500, Peninsula Labs). Secondary antibodies (Alexa Fluor, 1:400 dilution, Invitrogen) used were: goat (Gt) anti-chicken 488, Gt anti-rabbit 594 or 647, and Gt anti-mouse 594 or 647. Nuclear counterstain was performed using bisbenzimide.

Microscopy

Images were acquired with a Leica TCS SP5X confocal microscope. For confirmation of mCh and Prox1 co-localization in DGCs, images were acquired under a 63x objective at 1.0x optical zoom and 1 μm step size through the z-plane with the pinhole set at 1 Airy unit. For analysis of double-labeling for mCh and interneuron markers and quantification of mCh + cells, images were acquired with a 20x objective at 1.0x optical zoom and 2 μm step size through the z-plane with the pinhole set at 1 Airy unit.

Image Analysis and Statistics

Images were imported into Adobe Photoshop CS6 and analyzed for colocalization of immunoreactivity. Quantification was performed blinded to experimental group with coded images on sections spaced 480 μm apart that spanned the rostral-caudal extent of each hippocampus. Animals with a grossly damaged dentate gyrus were excluded. Within the dentate gyrus, birthdated starter DGCs were counted as cells that were GFP+/mCh+ and monosynaptic inputs as mCh+ only (GFP-negative) cells. Dentate hilar cells (including hilar ectopic DGCs) were defined as being at least two cell body widths away from the internal border of the granule cell layer. Identification of DGCs and interneurons was based on morphology, location and marker (Prox1, SST, PV) labeling. Cells that were both mCh+ and marker+ but GFP-negative were counted. We divided the number of mCh+/marker+ neurons by the number of starter neurons to calculate the average number of marker+ inputs per starter neuron. We also divided the number of mCh+/marker+ neurons by the total number of dentate gyrus mCh+ only neurons to yield the percentage of dentate gyrus inputs arising from a specific marker+ population. In hippocampal CA3 and CA1, identification and distinction of mCh+ only presynaptic interneurons and pyramidal cells were based on soma location and morphology. In the entorhinal cortex and subiculum, all mCh+ only inputs were counted without distinguishing between cell types.

Data for specific regions (i.e. CA3, CA1, EC and subiculum) were pooled between all immunostained sections/animal (≥36 sections) and normalized to the total GFP+/mCh+ starter DGCs within those sections. Statistical analyses were performed using GraphPad Prism 7 software. Group means were compared by one-way ANOVA and post-hoc Tukey's multiple comparisons test with significance level set at $p < 0.05$. All error bars represent SEM.

RESULTS

We combined the RbV-mediated retrograde trans-synaptic tracing technique[27] with RV reporter birthdating to map monosynaptic connections onto age-defined DGC populations in the intact or epileptic brain. RV-Syn-GTR was delivered to bilateral rat dentate gyri at either P7 or P60 to birthdate early-born or adult-born DGCs, respectively, and render them RbV infection-competent (Fig 1A, B). We induced SE at P56 and generated 4 cohorts of animals: epileptic animals that received RV at P60 (P60 SE), controls that received RV at P60 (P60 sham), epileptic animals that received RV at P7 (P7 SE), and controls that received RV at P7 (P7 sham). At 8–10 weeks after SE or sham treatment, RbV-mCh was injected into bilateral dentate gyri to selectively infect cells that were previously birthdated with RV-Syn-GTR through recognition of EnvA with TVA. In these GFP+/mCh+ 'starter cells,' RbV-mCh trans-complements with Rgp allowing it to travel retrogradely to label first-order presynaptic inputs of starter cells with mCh. These partner neurons lack Rgp and thus RbV-mCh cannot travel further (Fig 1A).

To first determine whether the RV-RbV system labels appropriate first-order DGC inputs, we examined monosynaptic inputs onto early- and adult-born DGCs in controls. We observed mCh+ cells exclusively in areas known to project onto DGCs, including local projections from the dentate hilus and long-distance afferents from the entorhinal cortex (EC), the

supramammillary nucleus (SUP), and the septum (Fig 1C, D; examples of dentate gyrus starter cells are yellow in the insets). Note that more mCh+ inputs were labeled for early-born DGCs (Fig 1C) than for adult-born DGCs (Fig 1D). This difference likely reflects more starter cells in P7 injected animals, consistent with the predominant neonatal generation of DGCs. Together, these findings support the feasibility of the dual-virus method for tracing monosynaptic inputs onto birthdated DGCs in the rat.

We next examined the local presynaptic inputs of adult-born DGCs in sham vs. epileptic rats, and the fidelity of RbV trans-synaptic retrograde labeling. After SE, as expected, the number of GFP+ adult-born DGCs increased vs. controls (Fig 2A, B) and many GFP+ hilar ectopic DGCs appeared, some of which were starter cells. In both cohorts, many mCh+/GFP- cells were present throughout the dentate gyrus (Fig 2A′, arrowheads in inset), representing local inputs onto GFP+/mCh+ starter DGCs (Fig 2A′, B′, arrows in inset). To eliminate possible RbV spread in the absence of RV-Syn-GTR, we injected P60 SE or sham rats with con-RV that that lacked Rgp, the protein necessary for RbV packaging and subsequent retrograde spread (Fig 2C, D). One week after RbV infection, we observed many starter DGCs (GFP+/mCh+) in sham and pilocarpine-treated animals with no evidence of mCh+ only presynaptic cells (Fig 2C′, D′).

After an epileptogenic insult, DGCs sprout mossy fibers into the inner molecular layer where they form functional synapses onto nearby DGCs.[5,23] We recently found that both early- and adult-born DGCs contribute to mossy fiber sprouting,[17] but it remains unclear whether these populations differ in the extent to which they *receive* mossy fiber innervation. We used the DGC marker Prox1 to quantify mCh+/Prox1+ (GFP-negative) cells, representing DGCs that monosynaptically innervate birthdated starter neurons. In animals that received RV-Syn-GTR at P60, we found mCh+/Prox1+/GFP- cells in the granule cell layer of both intact (Fig 3A, A′) and epileptic (Fig 3B, B′) rats. Notably, the mean number of presynaptic DGC inputs in the granule cell layer onto adult-born starter cells did not differ significantly between SE and sham groups (Fig 3E, GCL, P60 sham vs. P60 SE). When we examined presynaptic DGC inputs onto early-born DGCs in controls, we found significantly fewer DGCs that innervated early-born DGCs than adult-born DGCs under basal conditions (Fig 3C, C′ and E, left side, P60 sham vs. P7 sham). Our analysis also demonstrated that early-born DGCs received Prox1+ DGC presynaptic inputs after SE (Fig 3D, D′), and the amount per starter cell was not significantly different than the other 3 groups (Fig 3E). Intriguingly, despite the relatively low ratio of hilar ectopic to normotopic DGCs after SE, we observed significantly more mCh+/Prox1+/GFP- cells in the hilus of P60-injected animals after SE than in the other 3 groups, which represented hilar ectopic DGC inputs specifically onto adult-born DGCs (Fig 3B′, arrow and E, right side). Hilar ectopic DGC inputs onto P7 injected early-born DGCs were rare after SE (Fig 3D, D′ and E, right side).

We also analyzed the mCh+/Prox1+/GFP- proportion of all mCh+ non-starter cells in the dentate gyrus, which represented the proportion of all mCh+ only inputs that arose from presynaptic DGCs. We found that ~29% (25% from normotopic and 4% from hilar ectopic) of all dentate gyrus presynaptic inputs onto adult-born DGCs arose from other DGCs after SE vs. only ~5% in the intact brain (Fig 3F). Additionally, early-born DGCs after SE

received ~31% of their presynaptic inputs from other normotopic DGCs and less than 1% from hilar ectopic neurons, while early-born DGCs in the intact brain received only ~7% of inputs from other DGCs (Fig 3F). These results suggest that a greater proportion of dentate gyrus presynaptic inputs onto both DGC populations in the epileptic brain were from other DGCs. Moreover, some DGC-to-DGC connections arising after SE involved hilar ectopic DGC selectively synapsing onto adult-born DGCs. Because hilar ectopic DGCs arise only from adult-generated DGCs,[15] these data indicate that seizure-induced neurogenesis results in a specific recurrent excitatory network involving connections between ectopic and normotopic (or ectopic and ectopic) adult-generated neurons.

The SST-positive interneurons are susceptible to SE-induced death, but surviving SST+ interneurons sprout axon collaterals in the chronically epileptic brain.[24] To assess SST+ interneuron inputs onto birthdated DGCs, we triple labeled for GFP, mCh and SST (Fig 4A–D′). We found that both DGC populations in epileptic animals received fewer inhibitory inputs from SST+ interneurons vs. adult-born DGCs in controls, but not vs. early-born DGCs in controls (Fig 4E). In addition, more SST+ interneurons provided inputs onto adult-born DGCs vs. early-born DGCs in the intact brain (Fig 4E). When we calculated the percentage of all dentate gyrus mCh+/GFP- presynaptic inputs that arose from SST+ interneurons, we found that a smaller fraction of inputs onto early-born DGCs after SE arose from SST+ neurons vs. early-born DGCs in controls or adult-born DGCs in epileptic rats (Fig 4F).

To explore changes in PV+ interneurons, a population relatively less affected by SE-induced cell death,[30] we triple labeled for GFP, mCh and PV (Fig 5A–D′) and examined mCh+/PV+ cells. We calculated the mean number of mCh+/PV+ interneurons per starter DGC and found more mCh+/PV+ interneurons projecting monosynaptically onto adult-born DGCs in the intact brain vs. the other 3 groups (Fig 5E). No significant differences were observed in the ratio of mCh+/PV+ cells to all dentate gyrus mCh+ presynaptic inputs between any of the cohorts (Fig 5F). Together, these findings suggest that early-born DGCs in the epileptic brain are excessively disinhibited, while SST+ interneurons likely sprout preferentially onto adult-born neurons after SE. Moreover, adult-born DGCs in controls receive more inhibitory inputs than their early-born counterparts.

We next focused on potential inputs from hippocampal CA regions. Prior work supports the presence of intra-hippocampal projections into the dentate gyrus, particularly from CA3 pyramidal cells, under basal and pathological conditions.[20,31,32] Remarkably, we found evidence of robust connections directly onto DGCs, particularly after SE, with the presence of mCh+ cells in CA3 and CA1 (Fig 6A–L). We also found sparse mCh-labeled cells in area CA2 in all groups (data not shown). Presynaptic cells expressing mCh were present in all CA subregions in controls, and nearly all exhibited an interneuron morphology (Fig 6A, C). Although we found no significant differences in the mean number of CA3 mCh+ cells per starter cell between the four cohorts (Fig 6E), a much larger proportion of CA3 mCh+ inputs onto adult-born DGCs after SE arose from cells with pyramidal cell location and morphology (Fig 6B, D, F). Examination of CA1 showed significantly more mCh+ cells/starter cell in epileptic animals (Fig 6G–K), particularly for early-born DGCs (Fig 6K), and

more of these cells in both SE groups displayed a pyramidal neuron morphology and location than in controls (Fig 6L).

Evidence in the literature suggests that CA1 pyramidal cells innervate the dentate gyrus,[22,33,34] and recent work indicates that SST+ interneurons in CA1 sprout axon collaterals across the hippocampal fissure into the dentate gyrus after SE.[26] RbV tracing showed significant numbers of mCh+ processes that appeared to cross the hippocampal fissure in SE animals (Fig 6H, J, arrows). To further examine these projections, we injected a lentivirus carrying a CAMKIIα promoter driving a synaptophysin-GFP (CAMKIIα-Syp-GFP) fusion gene into CA1 of rats 3 weeks after SE or sham treatment to specifically label axonal projections of pyramidal neurons (Fig 6M). In controls, labeled CA1 pyramidal cell processes appeared in stratum radiatum and lacunosum moleculare, but largely respected the border of the hippocampal fissure and only rarely appeared to cross into the dentate gyrus (Fig 6N). In contrast, many more Syp-GFP-labeled processes in pilocarpine-treated rats appeared to cross the hippocampal fissure from CA1 into the dentate gyrus (Fig 6O, O′), supporting the potential of CA1 pyramidal neurons to innervate DGC dendrites after SE. Together, these findings suggest that substantial numbers of new excitatory feedback projections from CA3 and CA1 onto adult- and early-born DGCs arise in experimental mTLE.

To assess the major long-distance afferent pathway onto DGCs, the perforant path, we explored whether SE alters RbV labeling in the EC. We identified mCh+ presynaptic neurons in EC (Fig 7A–D) and quantified the average number of presynaptic inputs per starter cell. We found no statistically significant differences in the number of labeled EC neurons amongst the four groups (Fig 7E). We also found sparse inputs from the subiculum onto DGCs in all cohorts (Fig 7F–I) consistent with recent work describing these connections.[35] No statistically significant differences in the number of labeled subicular neurons were present between groups (Fig 7J).

DISCUSSION

Here we combine RV birthdating with RbV putative retrograde trans-synaptic tracing to identify changes in monosynaptic inputs onto age-defined DGC populations in the intact and epileptic brain. Our results suggest that adult- and early-born DGCs show similarities as well as distinct differences in seizure-induced plasticity in the epileptic hippocampus. We find that adult-born DGCs receive significant excitatory backprojections from CA3 pyramidal cells and substantial recurrent excitatory inputs from other DGCs. In particular, adult-born DGCs receive selective inputs from hilar ectopic DGCs, representing a novel recurrent excitatory pathway exclusively involving DGCs generated after SE. Interestingly, a significant proportion of presynaptic inputs onto early-born DGCs also arise from other DGCs after SE. Early-born DGCs are also preferential targets of CA1 pyramidal cell sprouting that likely involves pyramidal cell axons crossing the hippocampal fissure. In addition, early-born DGCs after SE display the least PV and SST inhibitory inputs, while SST+ interneurons likely sprout selectively onto adult-born DGCs.

We describe for the first time the finding that adult-born DGCs receive more recurrent excitatory inputs from hilar ectopic DGCs than do early-born DGCs that were mature at the time of SE. These changes may relate to the presence and positioning of persistent hilar basal dendrites on DGCs,[36] a seizure-induced pathology unique to adult-born DGCs.[13–15] Indeed, hilar basal dendrites are known to receive excessive excitatory synapses.[8,19] Moreover, as adult-born-DGCs undergo developmental synaptogenesis, they demonstrate enhanced plasticity[37,38] that likely heightens their potential for receiving new connections. While early-born DGCs in the epileptic brain appear to receive a similar proportion of all their presynaptic inputs from other DGCs as adult-born DGCs, the overall network-wide decrease in the number of inputs to early-born DGCs after SE makes DGC-to-DGC connections a more prominent proportion of their presynaptic inputs.

We also show that adult-born DGCs in the intact brain receive inputs from other DGCs to a much greater extent than early-born DGCs, suggesting that intrinsic differences exist between these two populations. This idea is contrary to the long-held belief that fully mature adult-born DGCs are functionally indistinguishable from their early-born counterparts. Timm staining to identify mossy fibers typically shows absent or minimal mossy fiber projections to the dentate inner molecular layer in intact rodents. While our work suggests that these connections exist, it is important to emphasize that they are relatively rare given the small number of adult-born neurons in intact animals compared with those after SE. Additionally, work using similar RbV tracing in mice suggests that DGCs synapse onto neighboring adult-born DGCs under normal, non-epileptic conditions.[33] Combined with our interneuron tracing findings, these results suggest that the innervation of adult-born DGCs differs from that of their early-born counterparts. In the future, modeling studies that take into account these differential connections may inform mechanisms by which adult-born DGCs contribute to pattern separation and pattern completion functions of the hippocampus.[39]

Importantly, we did not observe differences in the number of presynaptic DGC inputs onto adult-born DGCs in epileptic versus intact rats, which may seem counterintuitive to the notion that DGC-to-DGC connections increase onto adult-born DGCs after SE. However, based upon our data showing that DGC presynaptic inputs constitute a much smaller proportion of all inputs onto adult-born DGCs in controls, along with their lack of hilar ectopic DGC inputs, we reason that adult-born DGCs in the intact brain receive a significant amount of input from other cell types, most likely inhibitory interneurons, which counterbalances the increased DGC inputs.

The extensive inhibitory interneuron network in the dentate gyrus consists of a diverse population of cell types including two important subtypes: the SST+ and PV+ interneurons. Up to 83% of the inhibitory interneurons lost in the dentate gyrus after SE are SST+.[40] However, surviving SST+ interneurons hypertrophy and undergo axonal sprouting.[24,41] Our data suggest a loss of SST inputs onto early-born DGCs after SE, most likely due to SE-induced death, with preferential sprouting onto adult-born DGCs. Interestingly, the mean number of inputs from SST+ interneurons onto labeled DGCs is highest for adult-born neurons in controls. A potential reason for increased numbers of SST+ inputs onto adult- vs. early-born DGCs in the intact brain is that they may help counterbalance the excitatory DGC

inputs onto adult-born DGCs. An important caveat is that we cannot determine with these techniques whether a single SST+ interneuron is connected to one or multiple postsynaptic starter DGCs. Thus, it is possible that adult-born DGCs after SE receive similar numbers or even increased SST+ synapses compared to controls, but they simply arise from fewer SST+ cells. In contrast to the SST+ population, the PV+ interneurons are relatively resistant to SE-induced death[30] and we found similar numbers of PV+ inputs onto early-born DGCs in SE and control animals. Furthermore, we found more PV+ inputs onto adult-born than early-born DGCs in controls, similar to what was seen for SST+ inputs.

Hippocampal CA3 pyramidal cells are the main targets of DGC mossy fiber axons as part of the classic trisynaptic circuit. Previous work indicates low levels of CA3 backprojections onto DGCs, particularly at the CA3/hilar border, with most of the backprojecting cells identified as interneurons.[31,33,35] We found evidence of mostly CA3 inhibitory synapses onto DGCs under basal conditions. In the chronically epileptic brain, tracing studies suggest that CA3 pyramidal cells project axon collaterals into the dentate gyrus[42] and electrophysiological recordings reveal evidence of CA3 pyramidal cell to DGC connections.[20,32] Our data support and extend this work with the finding of extensive CA3 pyramidal cell backprojections onto adult-born DGCs, and to a lesser extent onto early-born DGCs, in the epileptic brain. The preferential targeting of CA3 pyramidal cell axons onto adult-born DGCs after SE may reflect the proximity of hilar ectopic DGCs or persistent hilar basal dendrites to backprojecting pyramidal cell axons.

Surprisingly, we found RbV-traced CA1 pyramidal cells, suggesting that they sprout axon collaterals across the hippocampal fissure to directly innervate DGCs. Although the finding was unexpected, rare monosynaptic connections from CA1 onto adult-born DGCs in intact mice have been reported in RbV tracing studies,[33] and CA1 pyramidal cells exhibit axonal sprouting in epilepsy models.[34,43–45] Recent work also indicates that SST+ interneurons in CA1 project axons across the hippocampal fissure to innervate DGCs in the mouse pilocarpine mTLE model.[26] We observed CA1 inputs preferentially onto early-born DGCs in epileptic rats. This selectivity may relate to the fact that, unlike DGCs generated after SE, dendrites of early-born DGCs already extend into the middle and outer molecular layers in the first few weeks after SE when much of the axonal reorganization is occurring.

The dentate ‘gate’ hypothesis proposes that the dentate gyrus acts as a gate that tempers hippocampal excitability through the relatively high threshold for DGC activation.[46] Previous work suggests that recurrent seizures in experimental mTLE may reflect breakdown of the dentate gate.[47,48] We found increased recurrent excitatory DGC-to-DGC inputs, increased recurrent backprojections from CA3 pyramidal cells onto adult-born DGCs, and increased CA1 pyramidal cell sprouting onto early- and adult-born DGCs after SE (Fig 8). These changes support a case for a breakdown of the dentate gate where excessive, aberrant excitatory connections lead to the development of seizures.

Some limitations of the present work warrant discussion. First, we were unable to identify RbV-labeled inputs from hilar mossy cells. This result is likely because hilar mossy cells are an extremely vulnerable population such that the RbV may have induced death of traced mossy cells rapidly after retrograde spread. While other groups have shown mossy cell

labeling in mouse RbV tracing studies,[49,50] species differences between rat and mouse (e.g., mossy cells express calretinin in mouse but not rat) may account for the discrepancy. Second, we cannot distinguish specific patterns of inputs onto normotopic vs. starter cells with aberrant morphology after SE. Targeting specific starter DGCs at a single cell level to trace inputs onto individual DGCs with differing seizure-induced morphology is a challenge for future work. Exploring other interneuron subtypes within the dentate gyrus not examined in this study, both within the dentate gyrus and the hippocampus proper, is also an important future direction. Regarding the specificity of RbV putative retrograde trans-synaptic tracing, evidence suggests that RbV travels across chemical synapses.[51–53] However, its mechanism of retrograde transport is still not fully understood and it remains possible that RbV spreads in other ways. Additionally, we most likely identified only a fraction of all the existing presynaptic inputs onto starter cells in our studies as we are limited by factors such as the amount of time before RbV begins to elicit cell death as well as less well-understood issues such as how retrograde spread is affected by neuronal subtype, synaptic density, strength and activity.[54] There is recent evidence that an improved glycoprotein may facilitate more robust retrograde spread of RbV[55] which may aid in identifying other inputs, particularly long-distance projections that were not characterized in detail in these studies.

In summary, our dual-virus tracing strategy provides unique insight into inherent differences in first-order presynaptic inputs onto adult- and early-born DGCs under both control and epileptic conditions. We identify novel connectivity as well as differences in existing inputs, and found that adult-born and early-born DGCs have unique properties and afferent connections that may contribute to aspects of epileptogenesis. An important focus for future studies is the functional consequences of these different inputs and how they alter network physiology. Such work should inform efforts for developing therapeutics that strategically target aberrant populations of DGCs for the treatment or prevention of mTLE.

Acknowledgments

We thank Ed Callaway and Fred Gage for providing viral constructs; Sam Pleasure for providing the Prox1 antibody; Andrew Tidball for generating the lentivirus; and Alison L. Althaus for her contribution to this work. We would like to acknowledge the use of the Microscopy and Image Analysis Laboratory (MIL) for preparation of confocal images. This study was supported by NS058585 (JMP), the Medical Scientist Training Program (XD), and an Epilepsy Foundation Predoctoral Research & Training Grant (XD).

References

1. Asadi-Pooya AA, Stewart GR, Abrams DJ, Sharan A. Prevalence and incidence of drug-resistant mesial temporal lobe epilepsy in the United States. World Neurosurg. 2016 Dec 26.
2. Wolf HK, Wiestler OD. Surgical pathology of chronic epileptic seizure disorders. Brain pathology. 1993 Oct; 3(4):371–80. [PubMed: 8293193]
3. Cavalheiro EA, Leite JP, Bortolotto ZA, Turski WA, Ikonomidou C, Turski L. Long-term effects of pilocarpine in rats: structural damage of the brain triggers kindling and spontaneous recurrent seizures. Epilepsia. 1991 Nov-Dec;32(6):778–82. [PubMed: 1743148]
4. Mello LE, Cavalheiro EA, Tan AM, et al. Circuit mechanisms of seizures in the pilocarpine model of chronic epilepsy: cell loss and mossy fiber sprouting. Epilepsia. 1993 Nov-Dec;34(6):985–95. [PubMed: 7694849]
5. Tauck DL, Nadler JV. Evidence of functional mossy fiber sprouting in hippocampal formation of kainic acid-treated rats. J Neurosci. 1985 Apr; 5(4):1016–22. [PubMed: 3981241]

6. Houser CR, Miyashiro JE, Swartz BE, Walsh GO, Rich JR, Delgado-Escueta AV. Altered patterns of dynorphin immunoreactivity suggest mossy fiber reorganization in human hippocampal epilepsy. The Journal of neuroscience : the official journal of the Society for Neuroscience. 1990 Jan; 10(1): 267–82. [PubMed: 1688934]
7. Parent JM, Yu TW, Leibowitz RT, Geschwind DH, Sloviter RS, Lowenstein DH. Dentate granule cell neurogenesis is increased by seizures and contributes to aberrant network reorganization in the adult rat hippocampus. The Journal of neuroscience : the official journal of the Society for Neuroscience. 1997 May 15; 17(10):3727–38. [PubMed: 9133393]
8. Ribak CE, Tran PH, Spigelman I, Okazaki MM, Nadler JV. Status epilepticus-induced hilar basal dendrites on rodent granule cells contribute to recurrent excitatory circuitry. J Comp Neurol. 2000 Dec 11; 428(2):240–53. [PubMed: 11064364]
9. Houser CR. Granule cell dispersion in the dentate gyrus of humans with temporal lobe epilepsy. Brain Res. 1990 Dec 10; 535(2):195–204. [PubMed: 1705855]
10. Parent JM, Elliott RC, Pleasure SJ, Barbaro NM, Lowenstein DH. Aberrant seizure-induced neurogenesis in experimental temporal lobe epilepsy. Annals of neurology. 2006 Jan; 59(1):81–91. [PubMed: 16261566]
11. von Campe G, Spencer DD, de Lanerolle NC. Morphology of dentate granule cells in the human epileptogenic hippocampus. Hippocampus. 1997; 7(5):472–88. [PubMed: 9347345]
12. Eriksson PS, Perfilieva E, Bjork-Eriksson T, et al. Neurogenesis in the adult human hippocampus. Nature medicine. 1998 Nov; 4(11):1313–7.
13. Jessberger S, Zhao C, Toni N, Clemenson GD Jr, Li Y, Gage FH. Seizure-associated, aberrant neurogenesis in adult rats characterized with retrovirus-mediated cell labeling. The Journal of neuroscience : the official journal of the Society for Neuroscience. 2007 Aug 29; 27(35):9400–7. [PubMed: 17728453]
14. Walter C, Murphy BL, Pun RY, Spieles-Engemann AL, Danzer SC. Pilocarpine-induced seizures cause selective time-dependent changes to adult-generated hippocampal dentate granule cells. The Journal of neuroscience : the official journal of the Society for Neuroscience. 2007 Jul 11; 27(28): 7541–52. [PubMed: 17626215]
15. Kron MM, Zhang H, Parent JM. The developmental stage of dentate granule cells dictates their contribution to seizure-induced plasticity. The Journal of neuroscience : the official journal of the Society for Neuroscience. 2010 Feb 10; 30(6):2051–9. [PubMed: 20147533]
16. Murphy BL, Pun RY, Yin H, Faulkner CR, Loepke AW, Danzer SC. Heterogeneous integration of adult-generated granule cells into the epileptic brain. J Neurosci. 2011 Jan 5; 31(1):105–17. [PubMed: 21209195]
17. Althaus AL, Zhang H, Parent JM. Axonal plasticity of age-defined dentate granule cells in a rat model of mesial temporal lobe epilepsy. Neurobiology of disease. 2016 Feb.86:187–96. [PubMed: 26644085]
18. Morgan RJ, Soltesz I. Nonrandom connectivity of the epileptic dentate gyrus predicts a major role for neuronal hubs in seizures. Proceedings of the National Academy of Sciences of the United States of America. 2008 Apr 22; 105(16):6179–84. [PubMed: 18375756]
19. Thind KK, Ribak CE, Buckmaster PS. Synaptic input to dentate granule cell basal dendrites in a rat model of temporal lobe epilepsy. J Comp Neurol. 2008 Jul 10; 509(2):190–202. [PubMed: 18461605]
20. Scharfman HE, Goodman JH, Sollas AL. Granule-like neurons at the hilar/CA3 border after status epilepticus and their synchrony with area CA3 pyramidal cells: functional implications of seizure-induced neurogenesis. J Neurosci. 2000 Aug 15; 20(16):6144–58. [PubMed: 10934264]
21. McAuliffe JJ, Bronson SL, Hester MS, et al. Altered patterning of dentate granule cell mossy fiber inputs onto CA3 pyramidal cells in limbic epilepsy. Hippocampus. 2011 Jan; 21(1):93–107. [PubMed: 20014385]
22. Smith BN, Dudek FE. Short- and long-term changes in CA1 network excitability after kainate treatment in rats. Journal of neurophysiology. 2001 Jan; 85(1):1–9. [PubMed: 11152700]
23. Buckmaster PS, Zhang GF, Yamawaki R. Axon sprouting in a model of temporal lobe epilepsy creates a predominantly excitatory feedback circuit. The Journal of neuroscience : the official journal of the Society for Neuroscience. 2002 Aug 1; 22(15):6650–8. [PubMed: 12151544]

24. Zhang W, Yamawaki R, Wen X, et al. Surviving hilar somatostatin interneurons enlarge, sprout axons, and form new synapses with granule cells in a mouse model of temporal lobe epilepsy. J Neurosci. 2009 Nov 11; 29(45):14247–56. [PubMed: 19906972]
25. Yu J, Proddutur A, Elgammal FS, Ito T, Santhakumar V. Status epilepticus enhances tonic GABA currents and depolarizes GABA reversal potential in dentate fast-spiking basket cells. Journal of neurophysiology. 2013 Apr; 109(7):1746–63. [PubMed: 23324316]
26. Peng Z, Zhang N, Wei W, et al. A reorganized GABAergic circuit in a model of epilepsy: evidence from optogenetic labeling and stimulation of somatostatin interneurons. The Journal of neuroscience : the official journal of the Society for Neuroscience. 2013 Sep 4; 33(36):14392–405. [PubMed: 24005292]
27. Wickersham IR, Lyon DC, Barnard RJ, et al. Monosynaptic restriction of transsynaptic tracing from single, genetically targeted neurons. Neuron. 2007 Mar 1; 53(5):639–47. [PubMed: 17329205]
28. Wickersham IR, Sullivan HA, Seung HS. Production of glycoprotein-deleted rabies viruses for monosynaptic tracing and high-level gene expression in neurons. Nature protocols. 2010 Mar; 5(3):595–606. [PubMed: 20203674]
29. Racine RJ. Modification of seizure activity by electrical stimulation. II. Motor seizure. Electroencephalogr Clin Neurophysiol. 1972 Mar; 32(3):281–94. [PubMed: 4110397]
30. Sun C, Mtchedlishvili Z, Bertram EH, Erisir A, Kapur J. Selective loss of dentate hilar interneurons contributes to reduced synaptic inhibition of granule cells in an electrical stimulation-based animal model of temporal lobe epilepsy. J Comp Neurol. 2007 Feb 10; 500(5):876–93. [PubMed: 17177260]
31. Li XG, Somogyi P, Ylinen A, Buzsaki G. The hippocampal CA3 network: an in vivo intracellular labeling study. J Comp Neurol. 1994 Jan 8; 339(2):181–208. [PubMed: 8300905]
32. Zhang W, Huguenard JR, Buckmaster PS. Increased excitatory synaptic input to granule cells from hilar and CA3 regions in a rat model of temporal lobe epilepsy. The Journal of neuroscience : the official journal of the Society for Neuroscience. 2012 Jan 25; 32(4):1183–96. [PubMed: 22279204]
33. Vivar C, Peterson BD, van Praag H. Running rewires the neuronal network of adult-born dentate granule cells. Neuroimage. 2016 May 1.131:29–41. [PubMed: 26589333]
34. Bausch SB, McNamara JO. Synaptic connections from multiple subfields contribute to granule cell hyperexcitability in hippocampal slice cultures. Journal of neurophysiology. 2000 Dec; 84(6): 2918–32. [PubMed: 11110821]
35. Bergami M, Masserdotti G, Temprana SG, et al. A critical period for experience-dependent remodeling of adult-born neuron connectivity. Neuron. 2015 Feb 18; 85(4):710–7. [PubMed: 25661179]
36. Spigelman I, Yan XX, Obenaus A, Lee EY, Wasterlain CG, Ribak CE. Dentate granule cells form novel basal dendrites in a rat model of temporal lobe epilepsy. Neuroscience. 1998 Sep; 86(1): 109–20. [PubMed: 9692747]
37. Schmidt-Hieber C, Jonas P, Bischofberger J. Enhanced synaptic plasticity in newly generated granule cells of the adult hippocampus. Nature. 2004 May 13; 429(6988):184–7. [PubMed: 15107864]
38. Ge S, Yang CH, Hsu KS, Ming GL, Song H. A critical period for enhanced synaptic plasticity in newly generated neurons of the adult brain. Neuron. 2007 May 24; 54(4):559–66. [PubMed: 17521569]
39. Deng W, Aimone JB, Gage FH. New neurons and new memories: how does adult hippocampal neurogenesis affect learning and memory? Nat Rev Neurosci. 2010 May; 11(5):339–50. [PubMed: 20354534]
40. Buckmaster PS, Jongen-Relo AL. Highly specific neuron loss preserves lateral inhibitory circuits in the dentate gyrus of kainate-induced epileptic rats. The Journal of neuroscience : the official journal of the Society for Neuroscience. 1999 Nov 1; 19(21):9519–29. [PubMed: 10531454]
41. Mathern GW, Babb TL, Pretorius JK, Leite JP. Reactive synaptogenesis and neuron densities for neuropeptide Y, somatostatin, and glutamate decarboxylase immunoreactivity in the epileptogenic

human fascia dentata. The Journal of neuroscience : the official journal of the Society for Neuroscience. 1995 May; 15(5 Pt 2):3990–4004. [PubMed: 7751960]

42. Siddiqui AH, Joseph SA. CA3 axonal sprouting in kainate-induced chronic epilepsy. Brain Res. 2005 Dec 20; 1066(1–2):129–46. [PubMed: 16359649]
43. Esclapez M, Hirsch JC, Ben-Ari Y, Bernard C. Newly formed excitatory pathways provide a substrate for hyperexcitability in experimental temporal lobe epilepsy. J Comp Neurol. 1999 Jun 14; 408(4):449–60. [PubMed: 10340497]
44. Perez Y, Morin F, Beaulieu C, Lacaille JC. Axonal sprouting of CA1 pyramidal cells in hyperexcitable hippocampal slices of kainate-treated rats. Eur J Neurosci. 1996 Apr; 8(4):736–48. [PubMed: 9081625]
45. Bausch SB, McNamara JO. Contributions of mossy fiber and CA1 pyramidal cell sprouting to dentate granule cell hyperexcitability in kainic acid-treated hippocampal slice cultures. Journal of neurophysiology. 2004 Dec; 92(6):3582–95. [PubMed: 15269228]
46. Lothman EW, Stringer JL, Bertram EH. The dentate gyrus as a control point for seizures in the hippocampus and beyond. Epilepsy Res Suppl. 1992; 7:301–13. [PubMed: 1334669]
47. Krook-Magnuson E, Armstrong C, Bui A, Lew S, Oijala M, Soltesz I. In vivo evaluation of the dentate gate theory in epilepsy. J Physiol. 2015 May 15; 593(10):2379–88. [PubMed: 25752305]
48. Heinemann U, Beck H, Dreier JP, Ficker E, Stabel J, Zhang CL. The dentate gyrus as a regulated gate for the propagation of epileptiform activity. Epilepsy Res Suppl. 1992; 7:273–80. [PubMed: 1334666]
49. Deshpande A, Bergami M, Ghanem A, et al. Retrograde monosynaptic tracing reveals the temporal evolution of inputs onto new neurons in the adult dentate gyrus and olfactory bulb. Proceedings of the National Academy of Sciences of the United States of America. 2013 Mar 19; 110(12):E1152–61. [PubMed: 23487772]
50. Vivar C, Potter MC, Choi J, et al. Monosynaptic inputs to new neurons in the dentate gyrus. Nature communications. 2012; 3:1107.
51. Ugolini G. Specificity of rabies virus as a transneuronal tracer of motor networks: transfer from hypoglossal motoneurons to connected second-order and higher order central nervous system cell groups. J Comp Neurol. 1995 Jun 05; 356(3):457–80. [PubMed: 7642806]
52. Tang Y, Rampin O, Giuliano F, Ugolini G. Spinal and brain circuits to motoneurons of the bulbospongiosus muscle: retrograde transneuronal tracing with rabies virus. J Comp Neurol. 1999 Nov 15; 414(2):167–92. [PubMed: 10516590]
53. Morcuende S, Delgado-Garcia JM, Ugolini G. Neuronal premotor networks involved in eyelid responses: retrograde transneuronal tracing with rabies virus from the orbicularis oculi muscle in the rat. The Journal of neuroscience : the official journal of the Society for Neuroscience. 2002 Oct 15; 22(20):8808–18. [PubMed: 12388587]
54. Callaway EM, Luo L. Monosynaptic Circuit Tracing with Glycoprotein-Deleted Rabies Viruses. The Journal of neuroscience : the official journal of the Society for Neuroscience. 2015 Jun 17; 35(24):8979–85. [PubMed: 26085623]
55. Kim EJ, Jacobs MW, Ito-Cole T, Callaway EM. Improved Monosynaptic Neural Circuit Tracing Using Engineered Rabies Virus Glycoproteins. Cell reports. 2016 Apr 13.

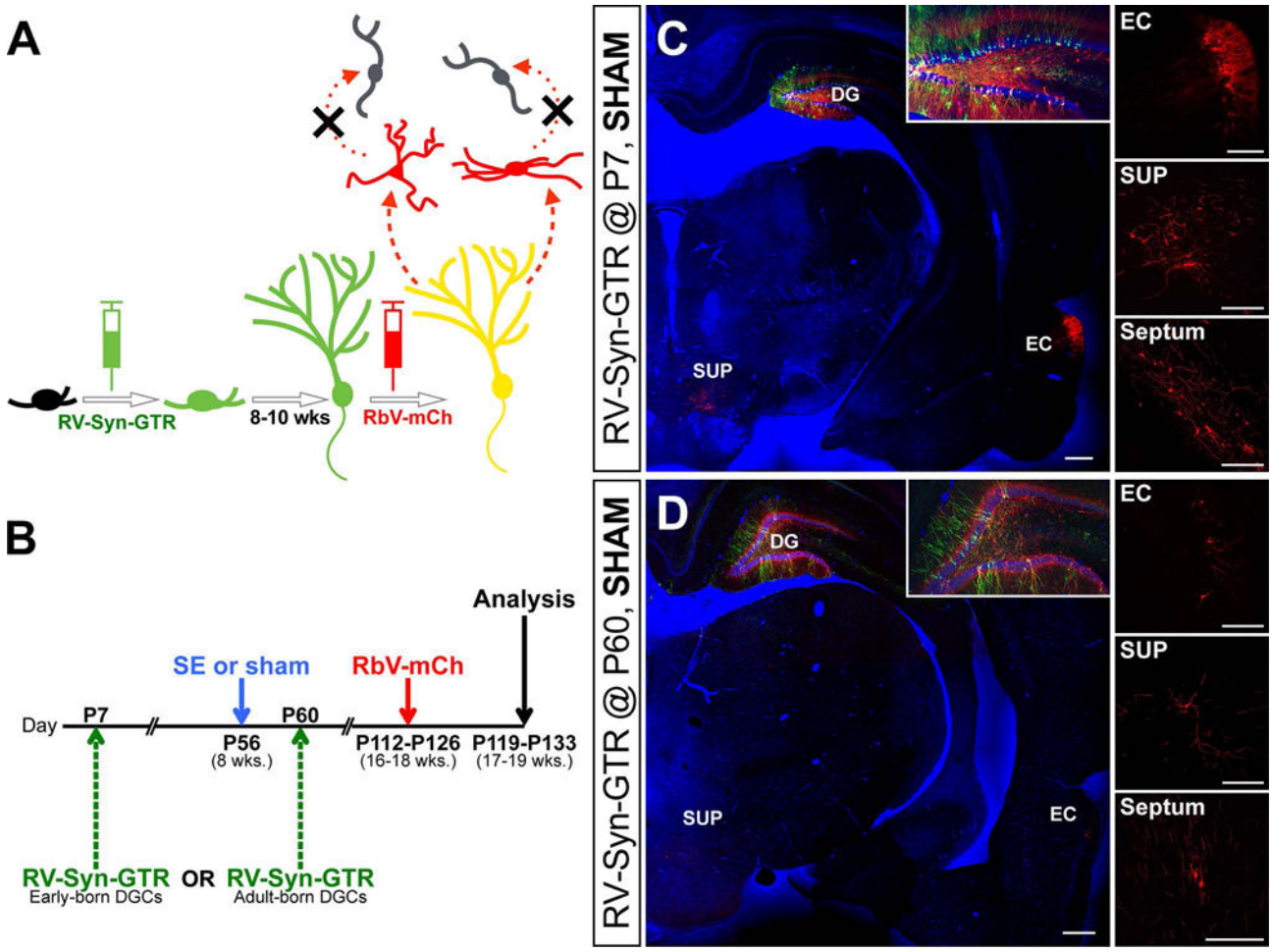

Figure 1. Dual virus tracing of presynaptic inputs onto early- and adult-born DGCs

A) RV-Syn-GTR injection into the dentate gyrus labels dividing DGC progenitors with GFP and also renders them competent for RbV-mCh infection 8–10 weeks later. The expression of Rgp by RV-Syn-GTR allows for RbV-mCh to travel retrogradely across only one synapse, thereby selectively labeling first-order presynaptic inputs with mCh. **B)** Experimental paradigm: RV-Syn-GTR is injected into bilateral dentate gyri at either P7 or P60 to birthdate early- or adult-born DGCs. Rats are treated with pilocarpine (SE) or vehicle (sham) at P56 and RbV-mCh is injected 8–10 weeks later. Animals are euthanized 1 week after RbV-mCh injection. **C**, **D)** Confocal images of brain slices showing dual-virus tracing of early- (**C**) and adult-born (**D**) DGCs in controls. There are presynaptic inputs from known areas that target DGCs such as the dentate hilus (insets), entorhinal cortex (EC), supramammillary nucleus (SUP), and septum (right panels). Note that GFP+/mCh+ (yellow) cells are ‘starter’ DGCs and their presynaptic inputs are mCh+ only. Bisbenzimide nuclear stain is shown in blue. Scale bars represent 100 μm (40 μm for insets).

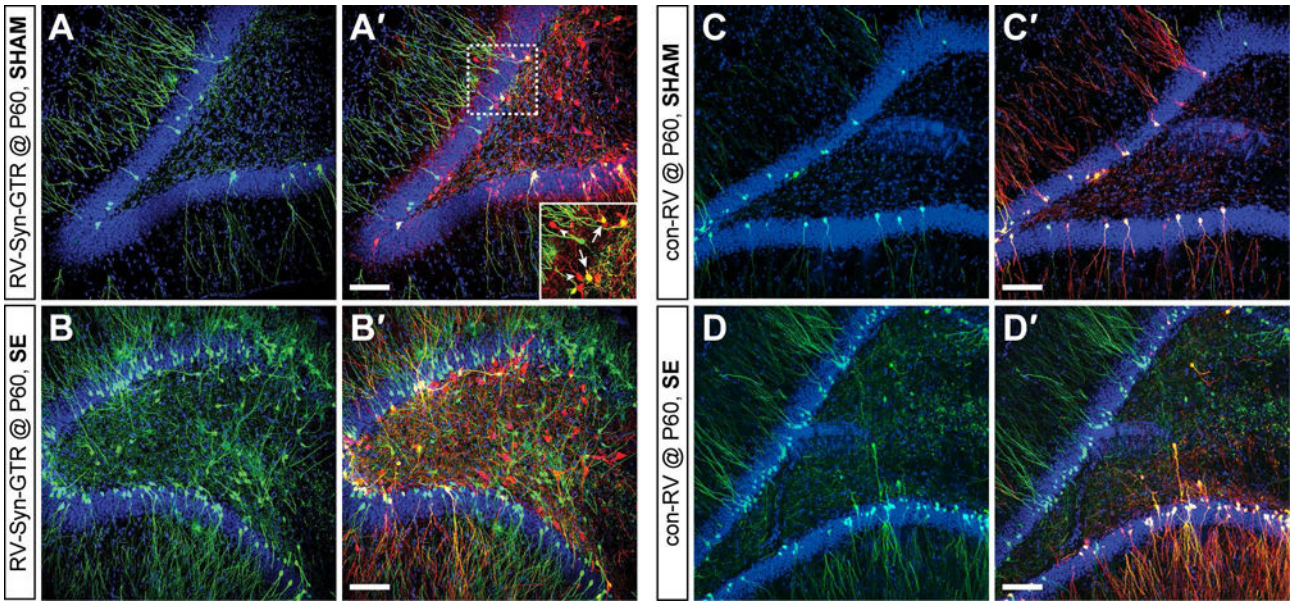

Figure 2. RbV-mCh retrograde spread in epileptic and control rats is dependent on the presence of Rgp

A) Confocal image of GFP labeling in the dentate gyrus of a control animal injected with RV-Syn-GTR at P60 to label adult-born DGCs. **A′**) GFP/mCh double labeling (same image as in **A**) showing that GFP+/mCh+ starter cells (arrows in inset) appear after RbV-mCh injection 8–10 weeks later, as well as traced mCh+ only presynaptic inputs (arrowheads in inset). **B)** Confocal image from a pilocarpine-treated rat injected with RV-Syn-GTR at P60 showing increased GFP labeling, including the appearance of GFP+ hilar ectopic adult-born DGCs. **B′**) RbV-mCh tracing (same image as in **B**) shows robust mCh+ only labeling in the hilus in addition to the presence of starter hilar ectopic GFP+/mCh+ DGCs. **C**, **D**) Confocal image of GFP labeling in the dentate gyrus after control RV (con-RV) was injected into sham or epileptic rats at P60. **C′**, **D′**) Without Rgp, RbV-mCh enters GFP+ cells to generate starter cells (yellow), but it cannot travel retrogradely as demonstrated by the lack of mCh+ only cells. Bisbenzimide nuclear stain shown in blue. Scale bars represent 100 μm (50 μm for inset).

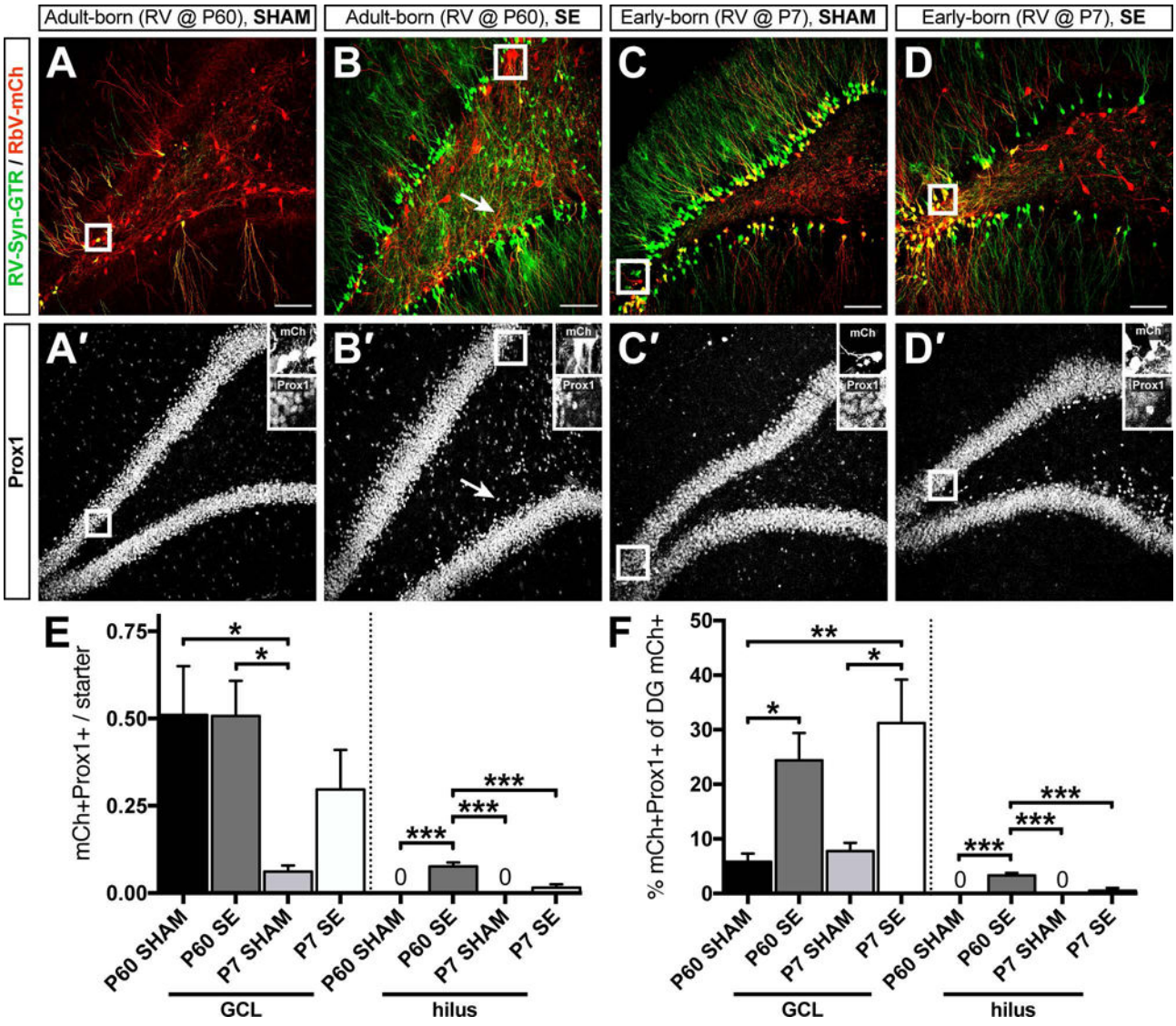

Figure 3. Prox1+ DGC inputs onto early- and adult-born DGCs differ in the sham vs. epileptic brain

A-D) Four cohorts of animals were used for the experimental paradigm. Representative confocal images of GFP/mCh double labeling in sham (**A**, **C**) and epileptic (**B**, **D**) dentate gyri that were injected with RV-Syn-GTR at P60 to label adult-born DGCs (**A**, **B**) or at P7 to label early-born DGCs (**C**, **D**). **A′-D′)** The same sections as in **A-D** labeled for Prox1 to identify DGCs (GFP and mCh were removed for clarity). Insets are high magnification images of mCh+ only cells that are also Prox1+ corresponding to the outlined areas in **A-D**. Arrows in **B** and **B′** show a traced mCh+ only/Prox1+ presynaptic hilar ectopic DGC. **E**) Quantification of average number of mCh+/Prox1+ (GFP-) presynaptic DGCs in the granule cell layer (GCL, left) and the hilus (right) per starter DGC. (**F**) Quantification of the percentage of all dentate gyrus mCh+ only inputs that were also Prox1+ in the granule cell layer (left) and the hilus (right). Scale bars represent 100 μm (50 μm for insets). (n = 5–6 animals per group, *p<0.05, **p<0.01, ***p<0.001).

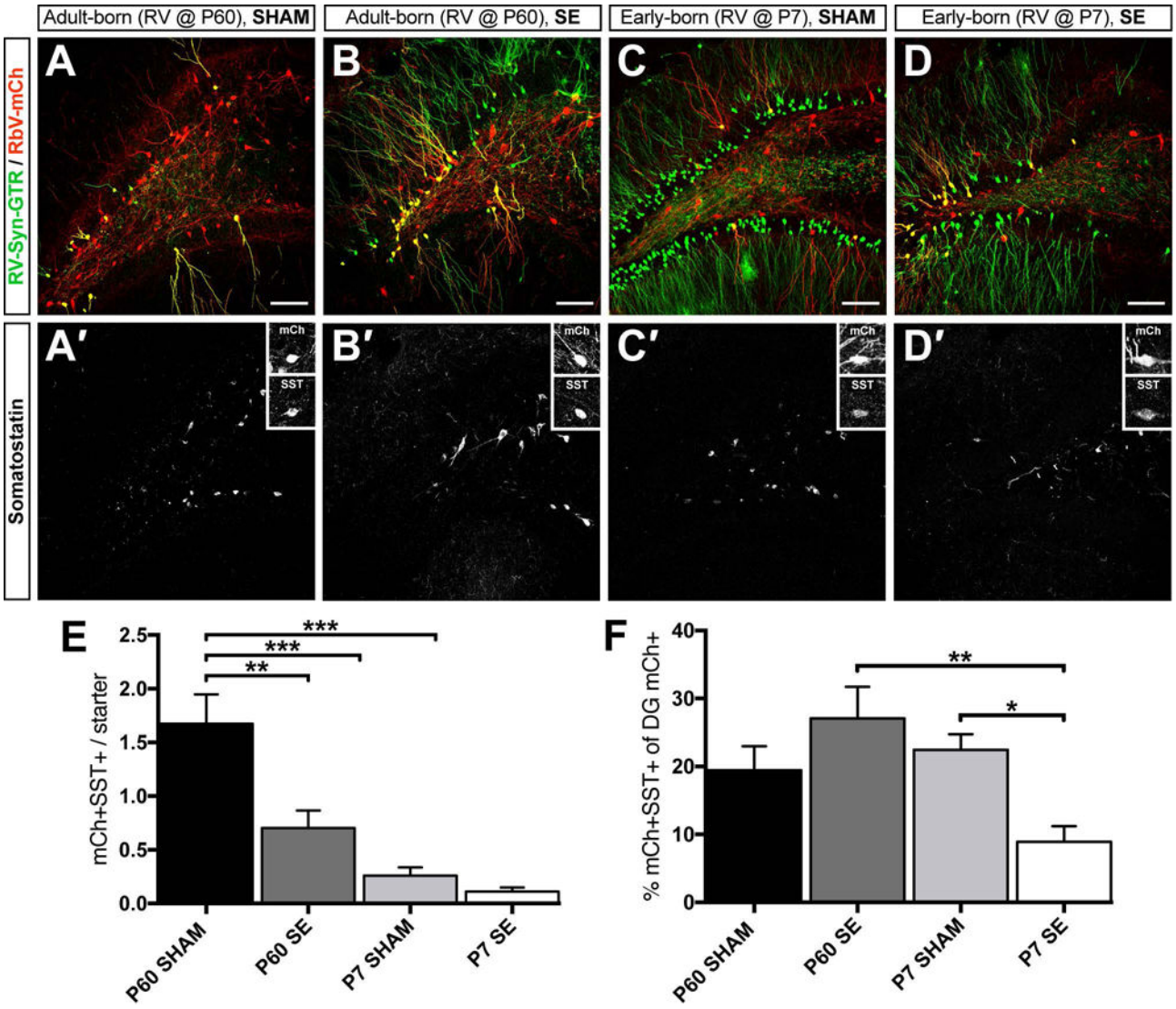

Figure 4. RbV tracing of hilar somatostatin+ interneuron inputs onto birthdated DGCs

A-D) Representative confocal images of the dentate gyrus from each of the four groups of animals immunolabeled for GFP and mCh. **A′-D′)** Triple labeling with SST in the same sections in **A-D** (GFP and mCh were removed for clarity). Insets show examples of mCh+ only traced inputs that were also SST+. Note that after SE, fewer SST+ cells are present but the surviving cells hypertrophy (**B′** and **D′**). **E)** Quantification of the mean number of mCh+ only presynaptic inputs that are also SST+ normalized to the number of starter cells. **F)** Quantification of the proportion of total dentate gyrus mCh+ only presynaptic inputs that are also SST+. Scale bars represent 100 μm (50 μm for insets). (n = 5–6 animals per group, *p<0.05, **p<0.01, ***p<0.001).

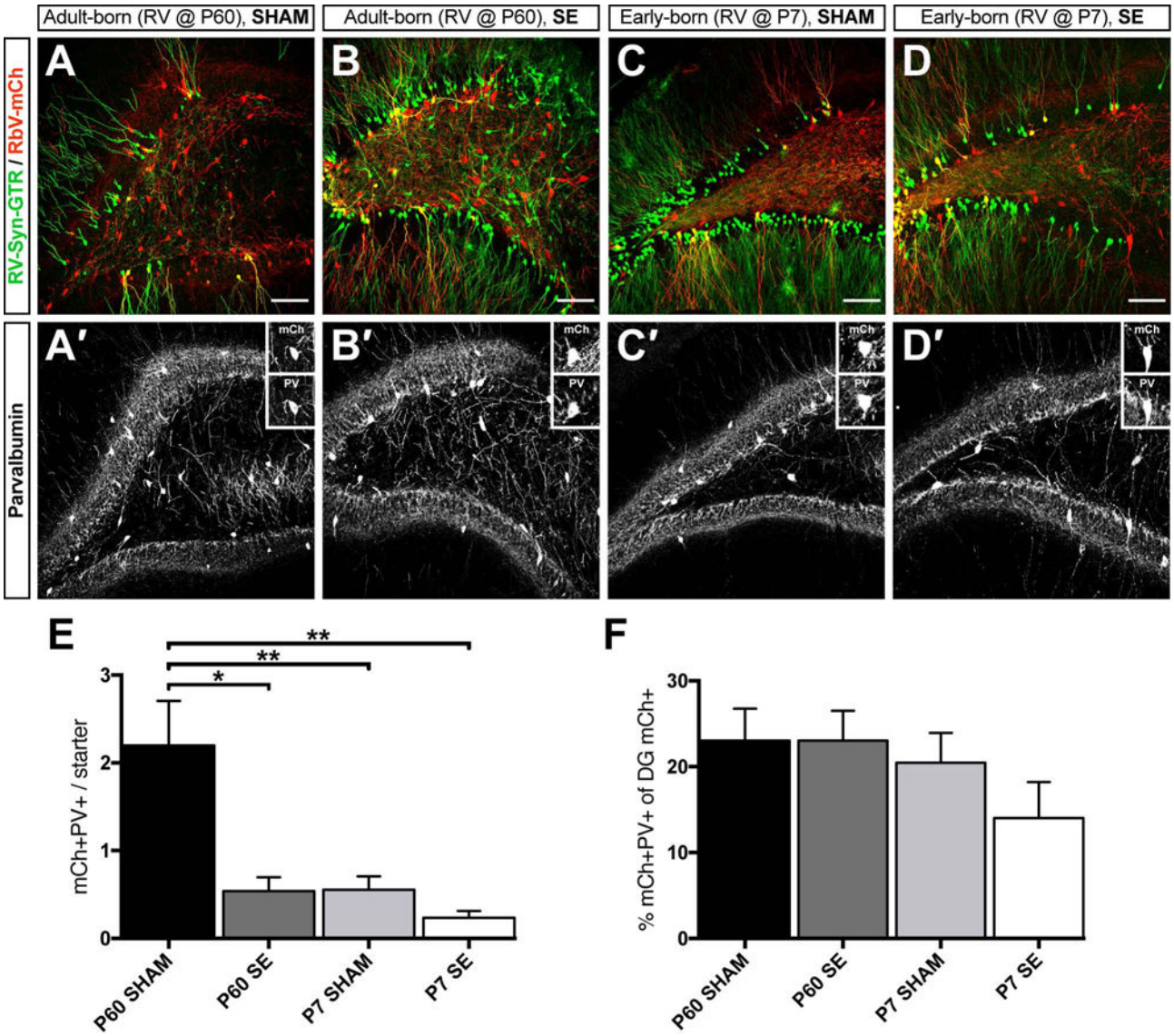

Figure 5. RbV tracing of dentate gyrus parvalbumin+ interneuron inputs onto birthdated DGCs

A-D) Representative confocal images of the dentate gyrus from each of the four groups of animals immunolabeled for GFP and mCh. **A′-D′)** Triple immunostaining with PV in the same sections in **A-D** (GFP and mCh were removed for clarity). Insets are high magnification views of mCh+ only cells that are also PV+. **E)** Quantification of the mean number of inputs from PV+ interneurons normalized to the number of starter cells. **F)** Quantification of the percentage of all dentate gyrus presynaptic mCh+ only inputs that are also PV+. Scale bars represent 100 μm (50 μm for insets). (n = 5–6 animals per group, *p<0.05, **p<0.01).

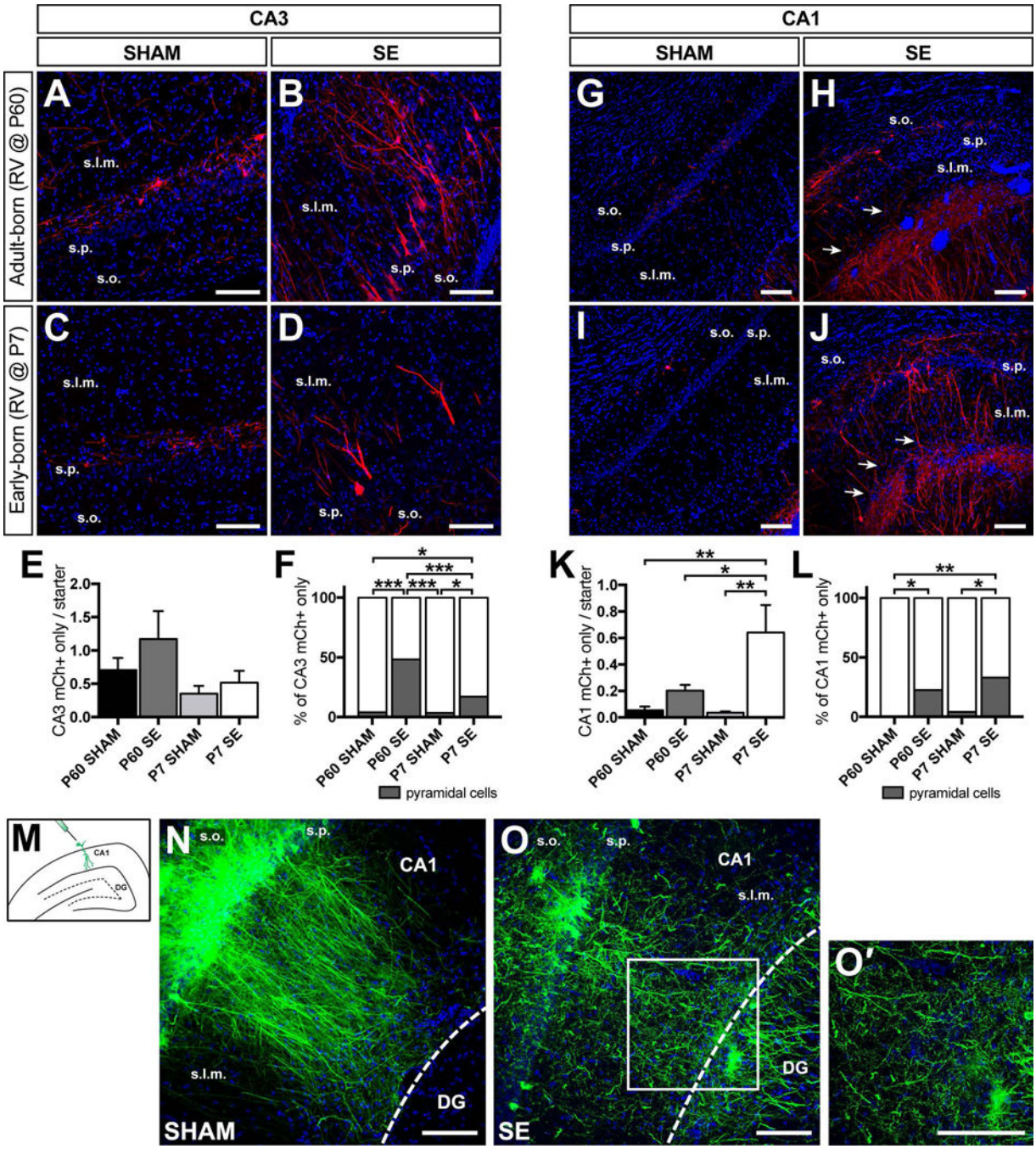

Figure 6. Hippocampal CA3 and CA1 pyramidal cells innervate DGCs in the epileptic brain

A-D) Representative confocal images of mCh immunolabeling of the hippocampal CA3 region for the four groups of animals. Note the increase in mCh+ cells with pyramidal neuron morphology within stratum pyramidale (s.p.) in the SE groups (**B**, **D**). **E)** Quantification of the ratio of total mCh+ only cells in CA3 to total starter DGCs amongst the four cohorts. **F)** Quantification of the percentage of all traced mCh+ only CA3 pyramidal vs. non-pyramidal cells. Dark grey represents pyramidal cells while white represents putative interneurons. **G-J)** Representative confocal images of mCh immunolabeling in the

CA1 region for the four groups. Note mCh+ fibers extending towards the dentate gyrus in epileptic rats (arrows in **H**, **J**). The dentate gyrus in at the lower right in **G-J**. **K)** Quantification of the ratio of mCh+ cells in CA1 to total starter DGCs in each group. **L)** Quantification of the percentage of all CA1 mCh+ only cells stratified into pyramidal vs. non-pyramidal cells. Dark grey represents the proportion of pyramidal cells while white represents putative inhibitory neurons. **M)** Schematic showing the location of the injection of CAMKIIα-Syp-GFP lentivirus. **N)** Representative confocal image of Syp-GFP labeled CA1 pyramidal cells from a sham animal. The dashed line represents the hippocampal fissure separating CA1 from the dentate gyrus (DG). Note that nearly all GFP+ processes terminate at the hippocampal fissure. **O)** Representative confocal image of Syp-GFP labeled CA1 pyramidal cells from an epileptic animal. Note the abundant processes from CA1 that appear to cross the hippocampal fissure (white dashed line) into the dentate gyrus. **O′)** Magnification of the region demarcated by the white solid box in **O.** Bisbenzimide nuclear stain in blue for all photomicrographs. Scale bars represent 100 μm. s.o., stratum oriens; s.p., stratum pyramidale; s.l.m., stratum lacunosum-moleculare. (n = 5–6 animals per group, *p<0.05, **p<0.01, ***p<0.001).

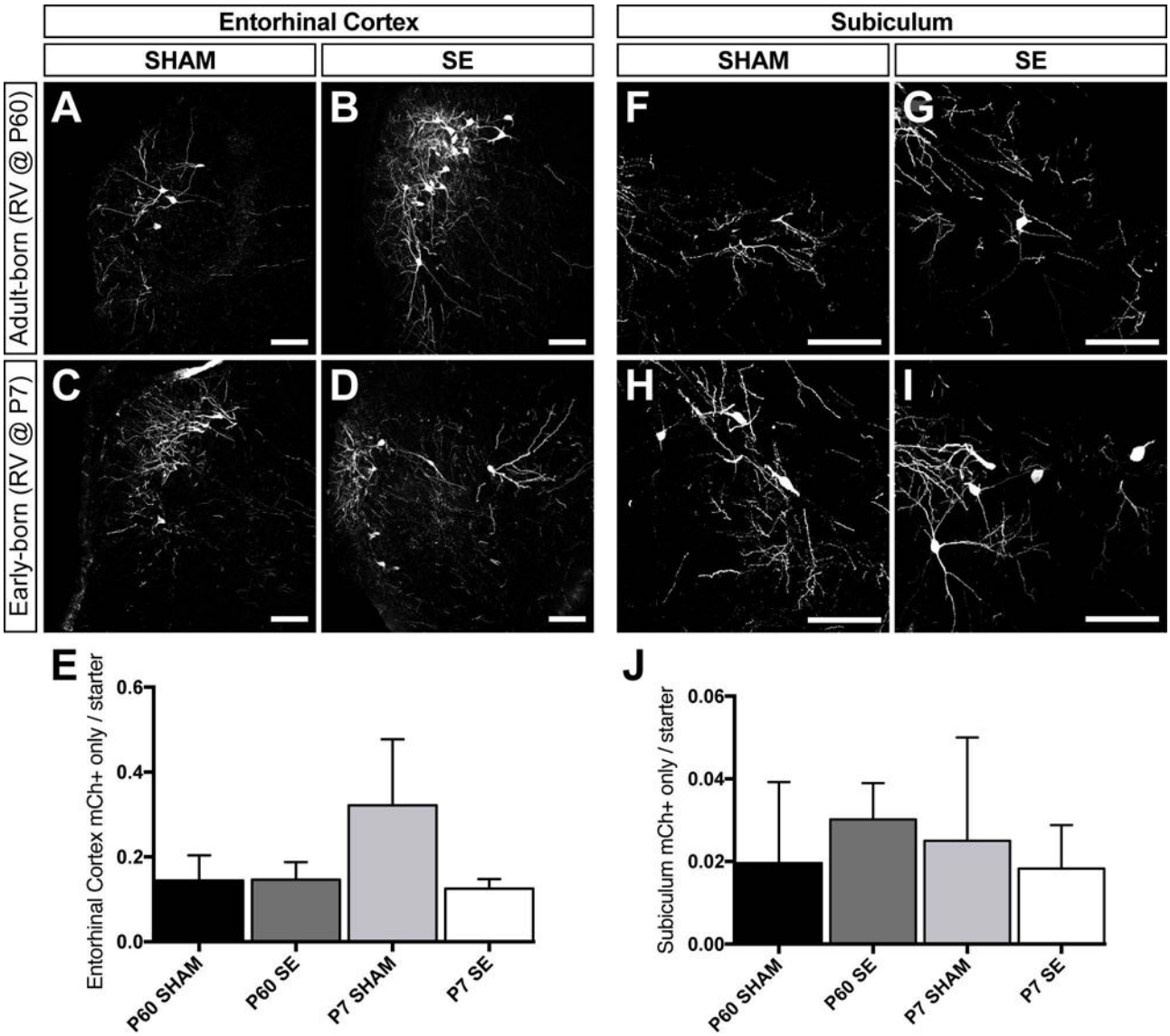

Figure 7. Quantification of entorhinal cortex and subicular inputs

A-D) Example images of inputs from the entorhinal cortex of all four groups. **E)** Quantification of mCh+ only inputs from the entorhinal cortex to the ratio of starter cells. **F-I)** Representative images of inputs from the subiculum of all four groups. **J)** Analysis of the ratio of mCh+ only subicular cells to the number of starter cells.

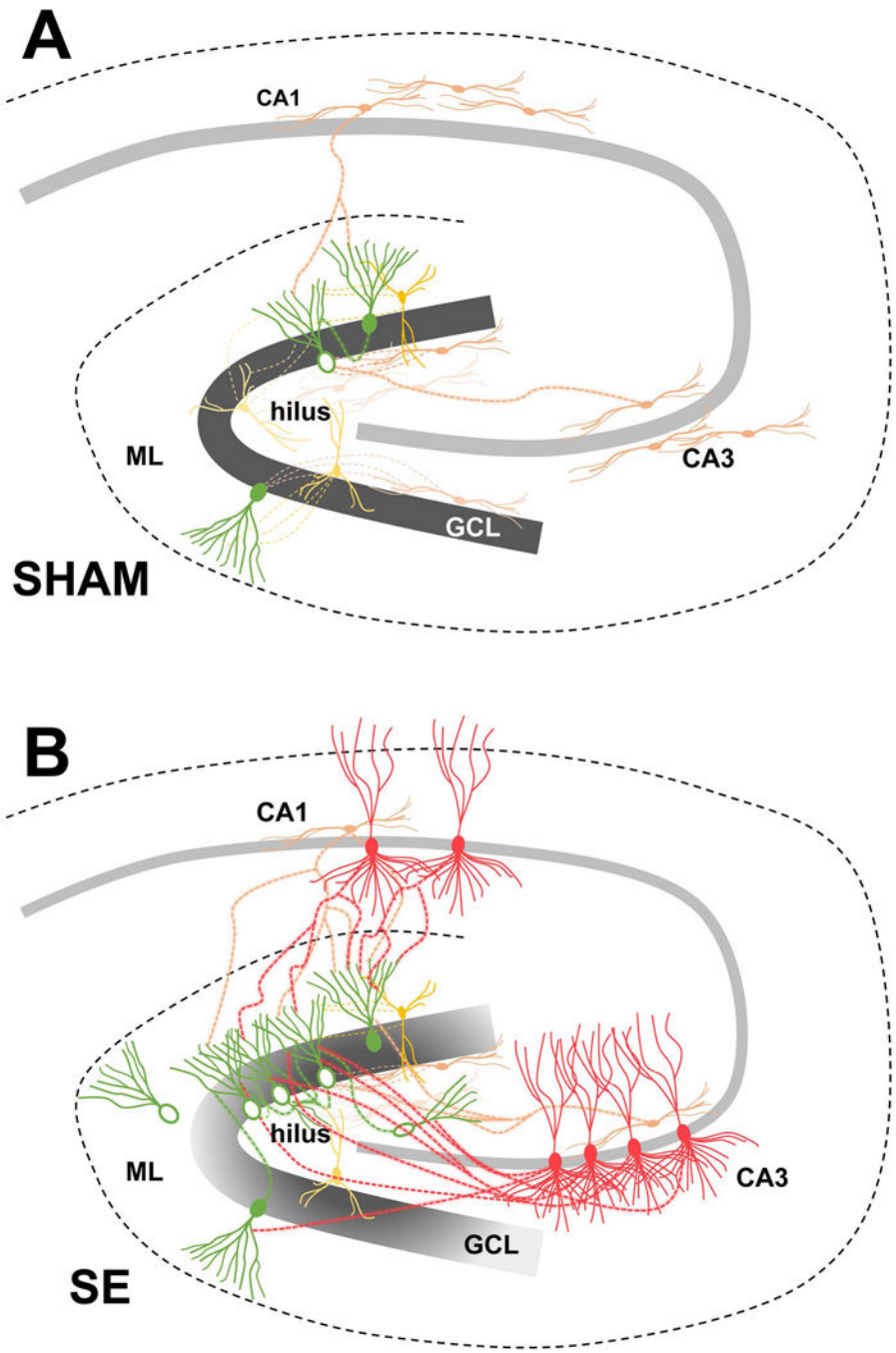

Figure 8. Hippocampal circuitry remodeling in the epileptic brain

A) Schematic of the control hippocampus displaying inhibitory inputs (yellow and orange) from the dentate hilus, CA3, and CA1 onto early- (filled green cell bodies) and adult-born (open green cell bodies) DGCs. Sparse DGC-DGC connections are also shown. **B)** Schematic of the epileptic brain demonstrating increased recurrent DGC-DGC connections onto both early- and adult-born DGCs after SE. Preferential inputs from hilar ectopic DGCs to adult-born DGCs also arise. CA3 pyramidal cells sprout axonal backprojections preferentially onto adult-born DGCs and CA1 pyramidal neurons project axons across the

hippocampal fissure onto early-born, and to a lesser extent, adult-born DGCs. ML, molecular layer; GCL, granule cell layer.